4 COMPUTATIONAL EVALUATION

4.1 Elastic Analysis

4.1.1 Aspect ratio studies

Shear locking was introduced in section 2.1.2 as a numerical issue where the Serendipity Mindlin element is concerned. This section evaluates extent of the shear locking problem and whether the issue is significant in the analysis of concrete slabs.

Shear locking causes an overestimation of plate stiffness for "thin" plates and it follows that plate thickness is the most significant factor influencing locking. Plates are therefore investigated over a range of span to thickness ratios.

The finite element analysis (FEA) mid-plate deflections of a simply supported and a clamped square plate, subjected to uniform transverse loading, are compared to the deflections obtained from classical methods. Navier's approach is used to calculate the exact plate deflection for the simply supported plate and Levy's solution is used for the clamped case, Ugural (1999). In both cases the Kirchhoff model of plate bending, i.e. thin plate theory, was employed. The resulting equations for a square plate are shown below:

$$w = 0.004066\frac{pl^4}{D} \text{ (simply supported)} \qquad (4.1)$$

$$w = 0.001264\frac{pl^4}{D} \text{ (clamped)} \qquad (4.2)$$

where p is the uniform load, l the plate length and

$$D = \frac{Eh^3}{12\left(1-\nu^2\right)} \qquad (4.3)$$

The finite element layout and boundary conditions are illustrated in figure 4-1 and the results of the study are plotted on figure 4-2 and figure 4-3. In the aforementioned figures, w_{FEA} denotes lateral deflection at the centre of the plate as calculated with the finite element method for two integration schemes and w_{KIR}, the lateral deflection as calculated with equations (4.1) and (4.2). The finite

element analysis employs Mindlin assumptions and the "exact" solutions employ Kirchhoff assumptions.

Clearly, numerical instabilities occur as the span to thickness ratio becomes large, regardless of the integration scheme employed. Reduced integration improves the performance of the element, but does *not* eliminate locking. For the serendipity element a 3x3 point Gaussian quadrature is exact, whereas a 2x2 point quadrature is a reduced integration scheme.

Although this finding is significant in analyses dealing with thin plates, reinforced concrete slabs rarely exhibit span to thickness ratios larger than 32. This ratio is represented by the vertical line in figure 4-2 and figure 4-3. As can be seen from these figures the deflection is at least overestimated, if not entirely accurate for ratios smaller than 32, even with exact integration.

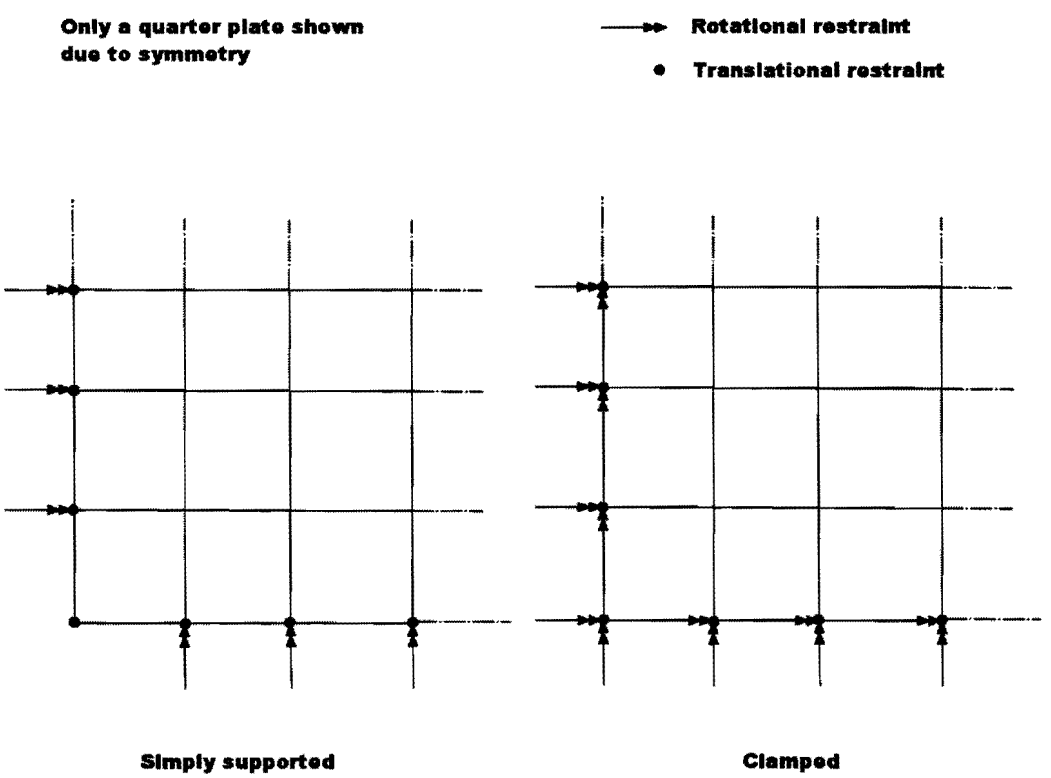

Figure 4-1: Element layout and boundary conditions

4.1.2 Convergence Studies

An issue that often arises in a finite element analysis is that of mesh density. The analyst always attempts to use the least number of elements and still obtain reliable results. This section studies various mesh densities on plates subjected to uniform loading in an attempt to find the optimum number of elements on a rectangular grid for slab problems.

The simply supported and clamped square plates illustrated in figure 4-1 are used with a varying number of elements. The plate analysed is a 6m square plate, 600mm thick subjected to a 5kPa distributed load. Both the Mindlin and Kirchhoff models for plate bending are used for analytical comparison. The analytical results for maximum deflection using the Kirchhoff assumptions are given in equations (4.1) through (4.3) and the results for the Mindlin model are given below, Liu (2002):

$$w = 0.00427\frac{pl^4}{D} \text{ (simply supported)} \qquad (4.4)$$

$$w = 0.0015\frac{pl^4}{D} \text{ (clamped)} \qquad (4.5)$$

where all variables are as defined in section 4.1.1.

As can be seen from figure 4-4 and figure 4-5, very little is gained from a mesh finer than 6x6, as far as accuracy is concerned. One should note that this result is valid for square plates subjected to uniform pressures only.

The curves labelled *Mindlin* plot the ratio of w_{FEA}/w_{exact}, where w_{exact} is calculated using equations (4.4) and (4.5). The curves labelled *Kirchhoff* uses a w_{exact} calculated from equations (4.1) and (4.2), w_{FEA} refers to the results of a finite element analysis (Mindlin assumptions, and 2x2 integration) throughout.

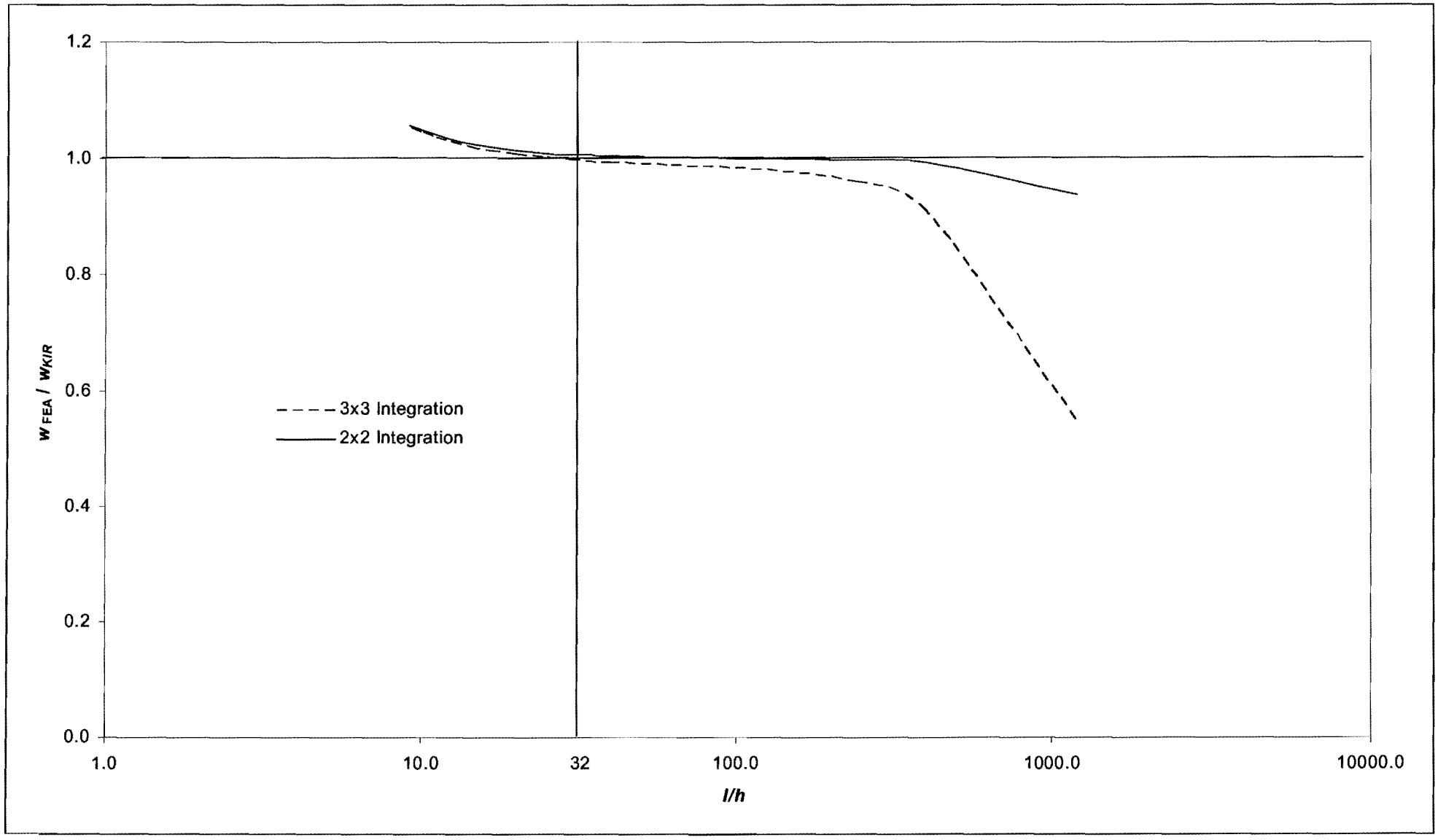

Figure 4-2: Aspect ratio study for a simply supported square plate

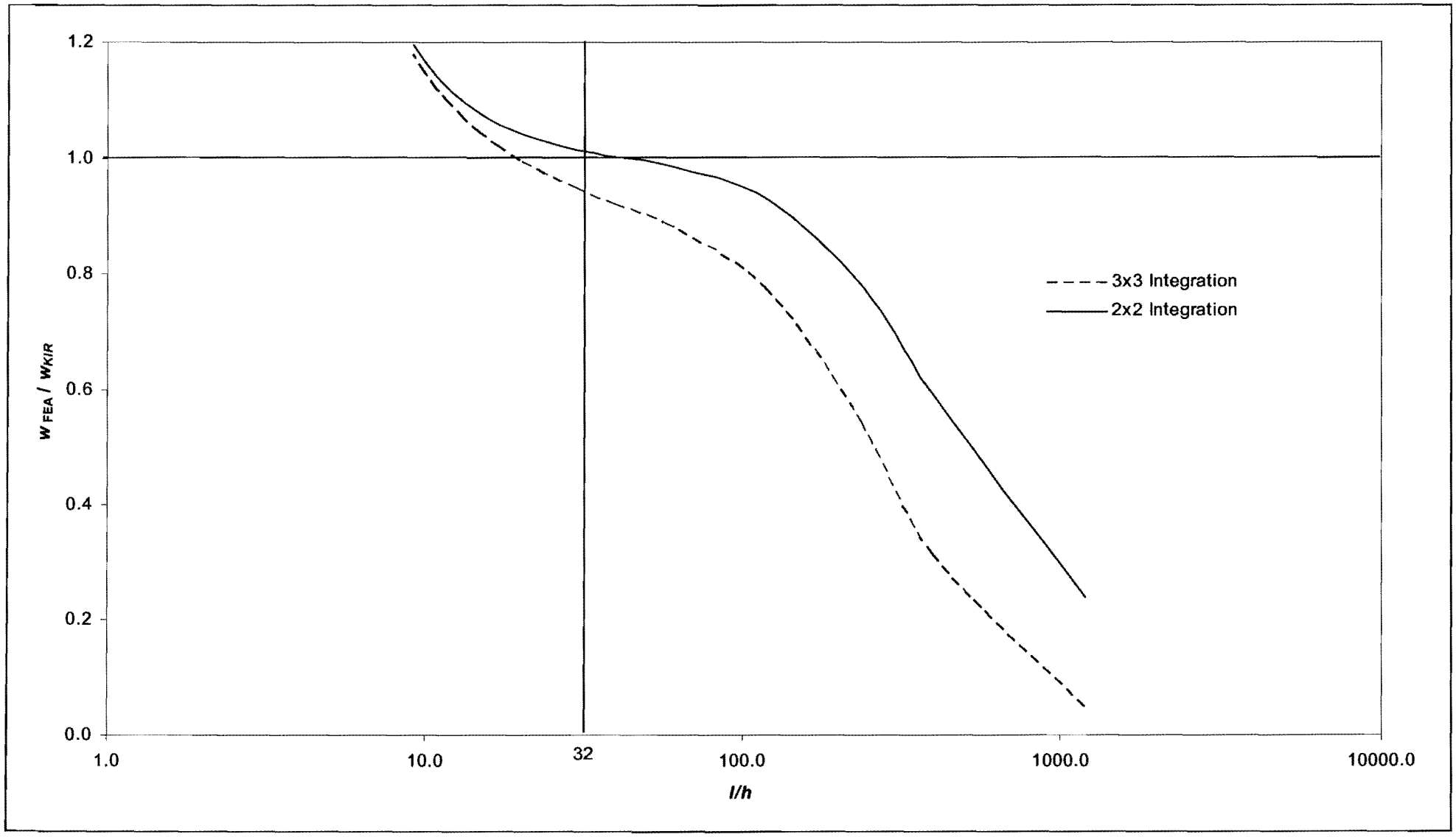

Figure 4-3: Aspect ratio study for a clamped square plate

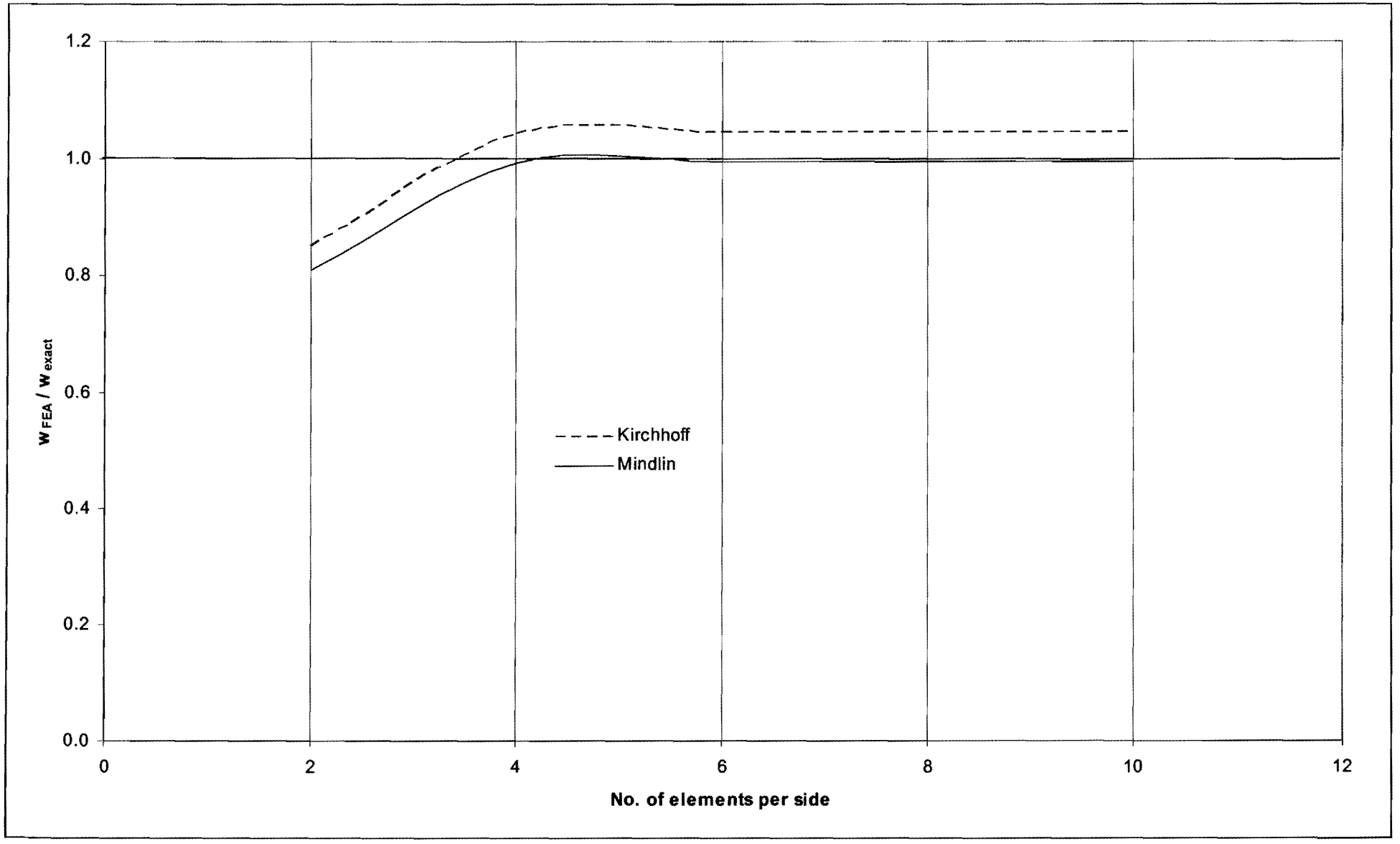

Figure 4-4: Convergence study for a simply supported square plate

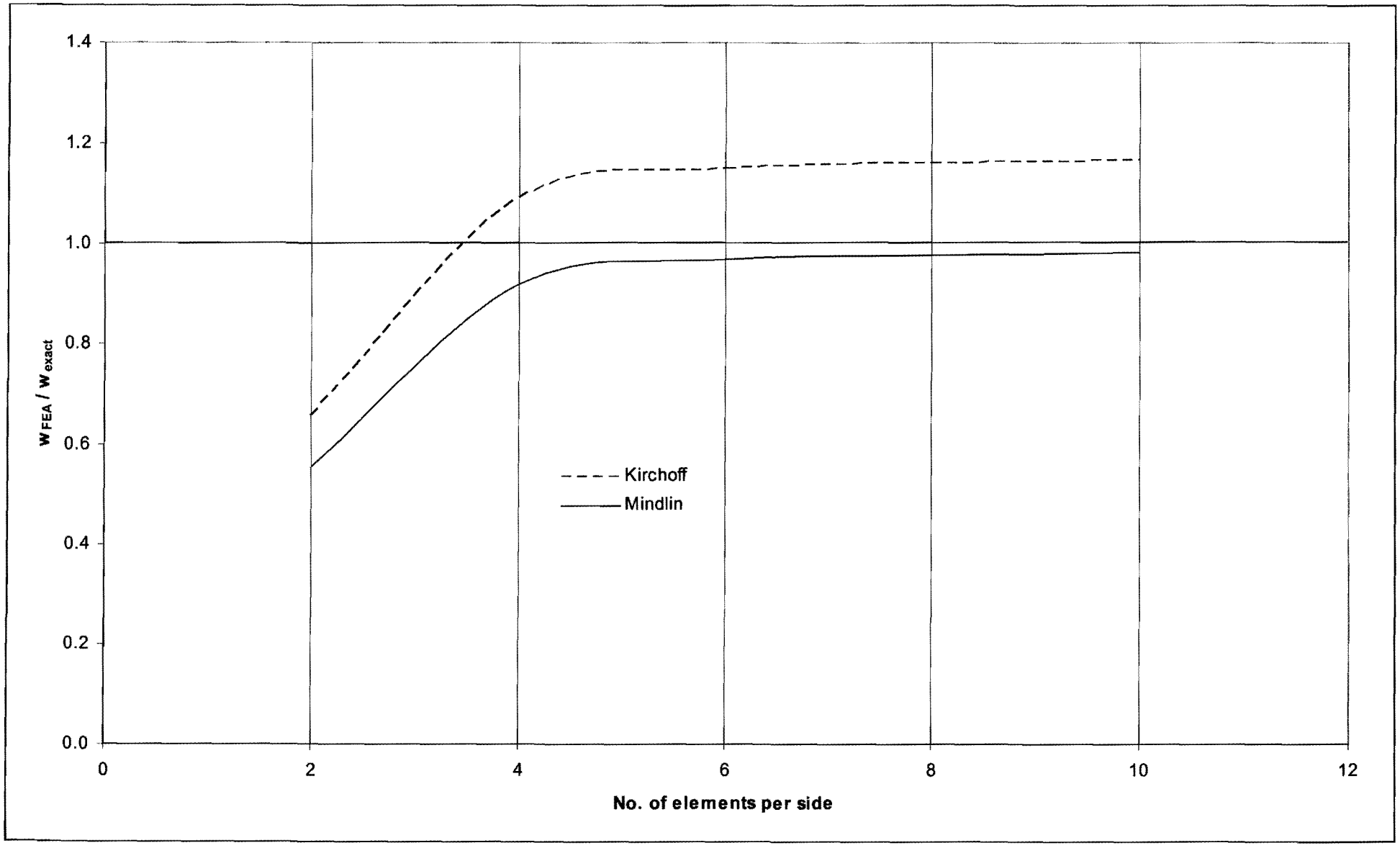

Figure 4-5: Convergence study for a clamped square plate

It is interesting to note that the element deteriorates in the case of the clamped plate, this indicates that the influence of shear deformation on flexural deflections of a plate is not solely dependent on the span to depth ratio, but also on boundary conditions.

4.2 Polak Slab Specimen

A slab tested by Polak (1994) was used to corroborate the results yielded by the effective stiffness method presented in section 2.2.2. The data from these slabs are used in this section to verify the software developed by the author and to test the applicability of the tension stiffening method presented in sections 2.2.1 and 3.1.

The specimen employed for comparison, labelled SM1, is illustrated in Table 4-1 and figure 4-6.

Dimensions (mm)	E_c **(GPa)**	ρ_x*	ρ_y*	d_x **(mm)**	d_y**(mm)**	ν
1625 x 1625 x 316	34.278	1.25%	0.42%	281	256	0.2

Table 4-1: Specimen properties (*per layer)

Specimen SM1, simply supported on two opposite edges, was loaded with uniaxial moments on the supported edges. The loading conditions and finite element model for the slab are shown in figure 4-6 and figure 4-7.

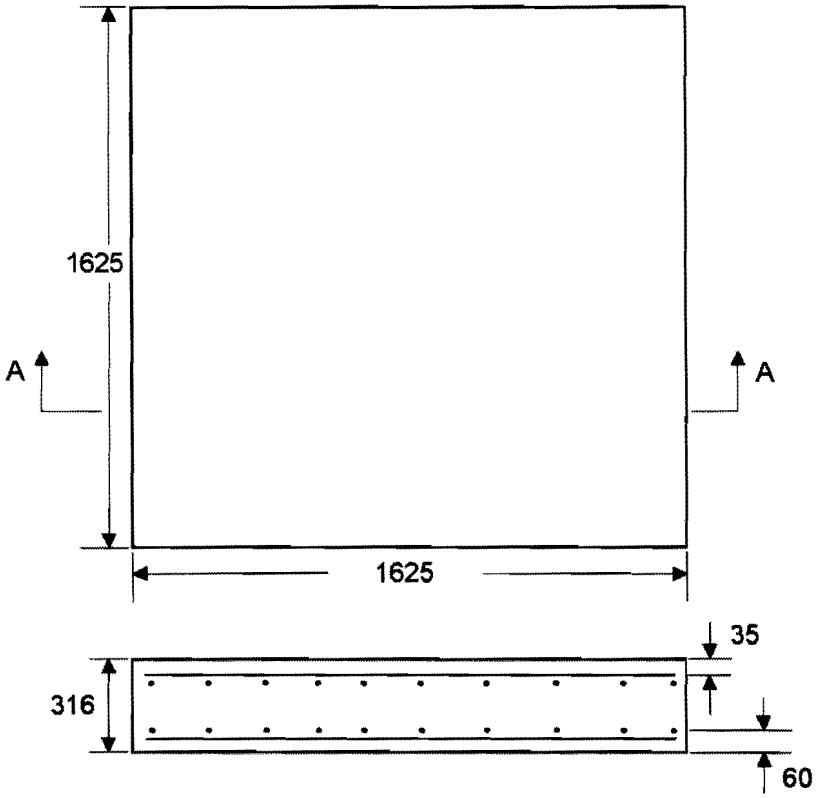

Figure 4-6: Specimen Geometry and Reinforcement

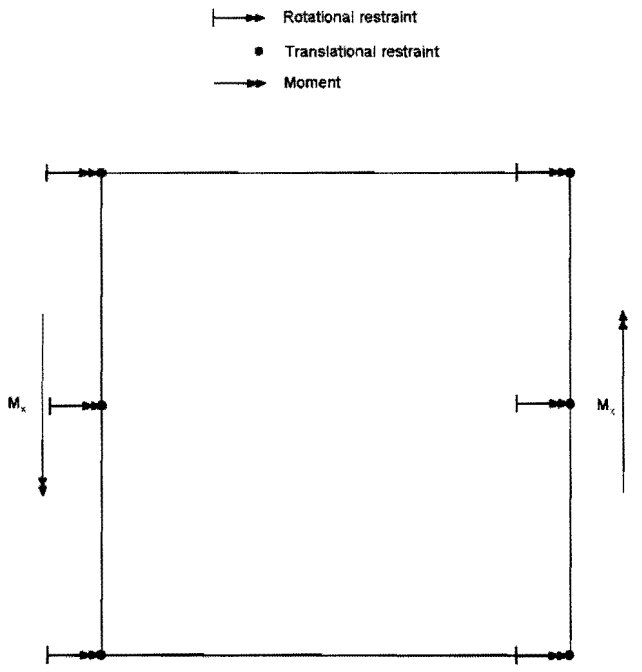

Figure 4-7: Finite element model for specimen SM1

A comparison of the results of the experimental and numerical analysis of specimen SM1 are plotted in figure 4-10. It is evident from figure 4-10 that the author's implementation of both the Bilinear and Branson's approach to tension stiffening compares favourably with the experimental data of specimen SM1 and the results of Polak.

4.3 Jofriet & McNeice Slab

Jofriet and McNeice (1971) performed a point loading test on a corner supported slab, the properties of which are indicated in Table 4-2. The point load was applied to the centre of the slab.

Dimensions (mm)	E_c **(GPa)**	ρ_x	ρ_y	$d_{x,y}$**(mm)**	ν
914 x 914 x 44	28.623	0.85%	0.85%	33	0.15

Table 4-2: Specimen properties

The specimen geometry is illustrated in figure 4-8 and the finite element model in figure 5-9.

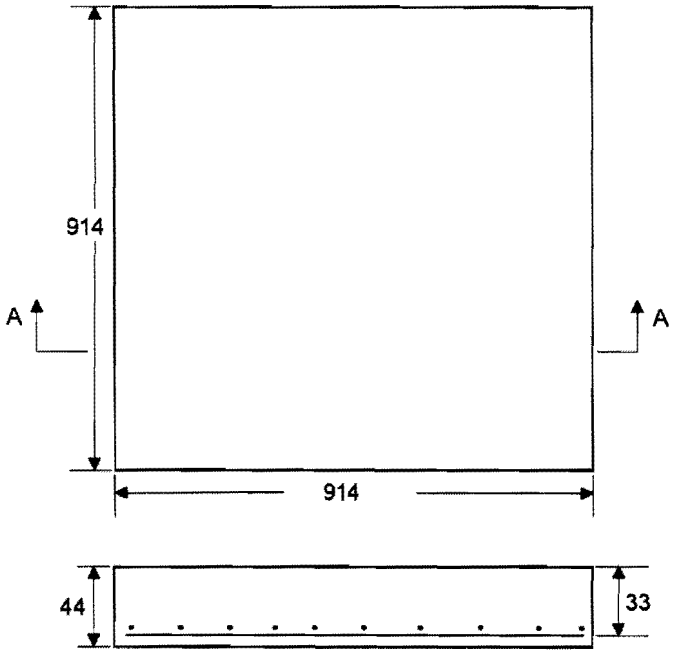

Figure 4-8: Specimen Geometry and Reinforcement

The slab model consists of a 6x6 mesh with the translational degrees of freedom restrained at the corner nodes. The slab was subjected to a central point load and deflections measured at point A as indicated. With the element mesh as shown, this point fortuitously coincides with a mid-edge node of a central element.

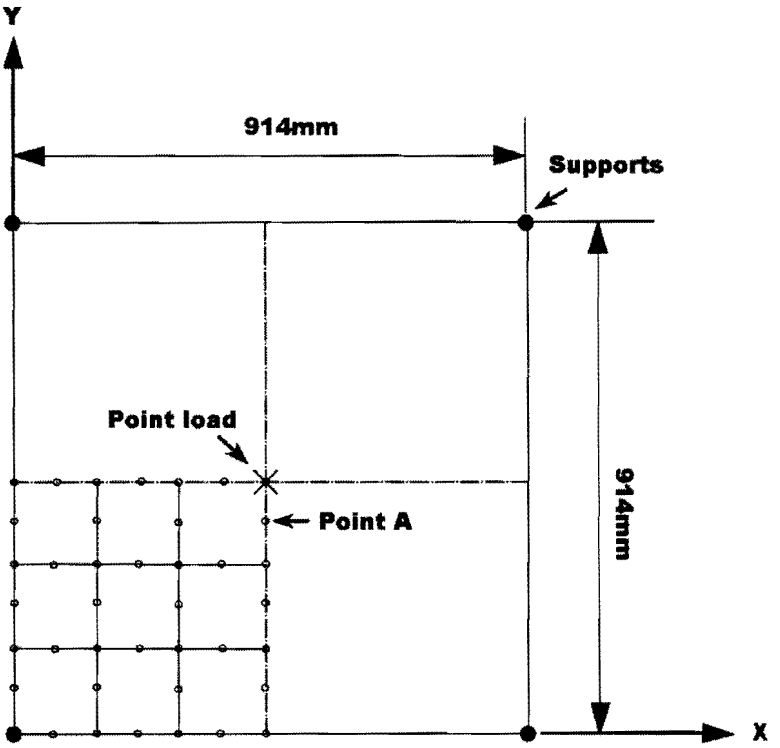

Figure 4-9: Jofriet and McNeice slab model

The results of both Polak and the author's analysis are plotted against the experimental data of Jofriet and McNeice in figure 4-11. It should be noted that Branson's approach yields results far superior to the bilinear approach. Careful investigation of the parameters influencing these two methods reveals that the bilinear method is very sensitive to changes in reinforcement ratio.

The curve of the effective moment of inertia versus applied moment curve changes shape with lower reinforcement ratios when using the Bilinear method, whereas the curves retain a similar shape when using Branson's method, see figure 4-12 for details. The figure implies that the bilinear method becomes unreliable with lower reinforcement ratios. This finding casts significant doubt on the usefulness of bilinear method in flat slab problems where reinforcement ratios are typically fairly low.

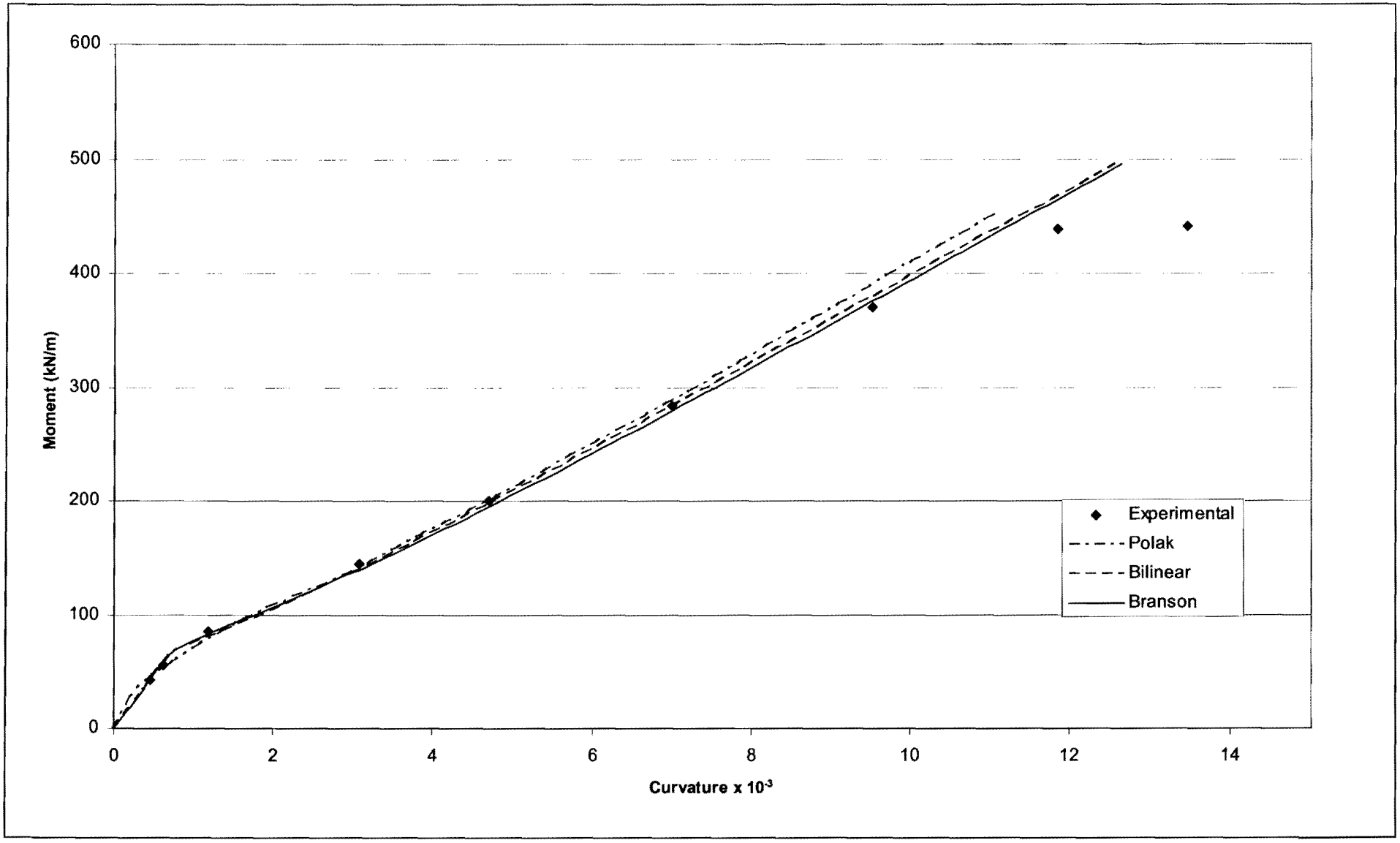

Figure 4-10: Specimen SM1 analysis results

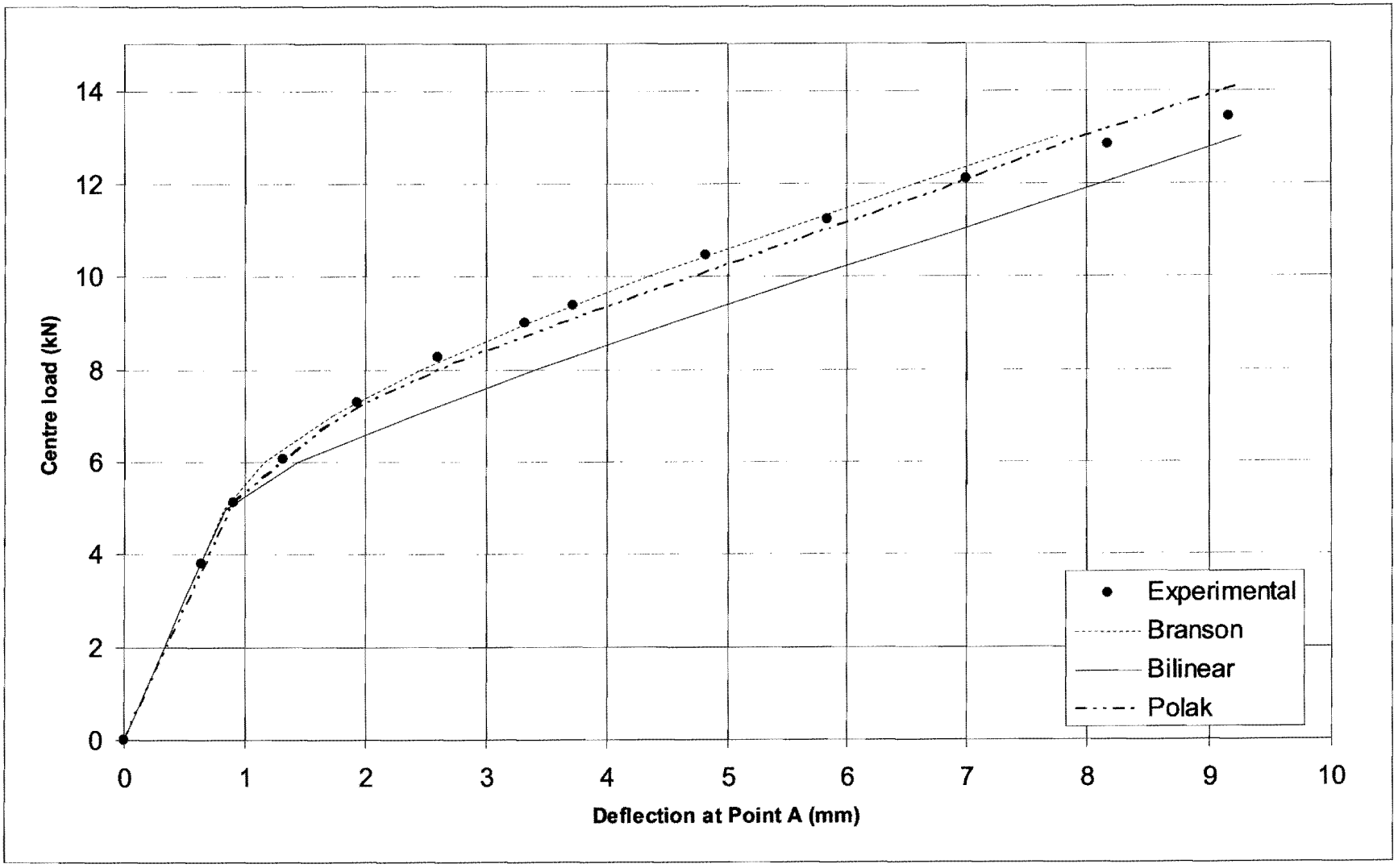

Figure 4-11: Jofriet and McNeice slab results

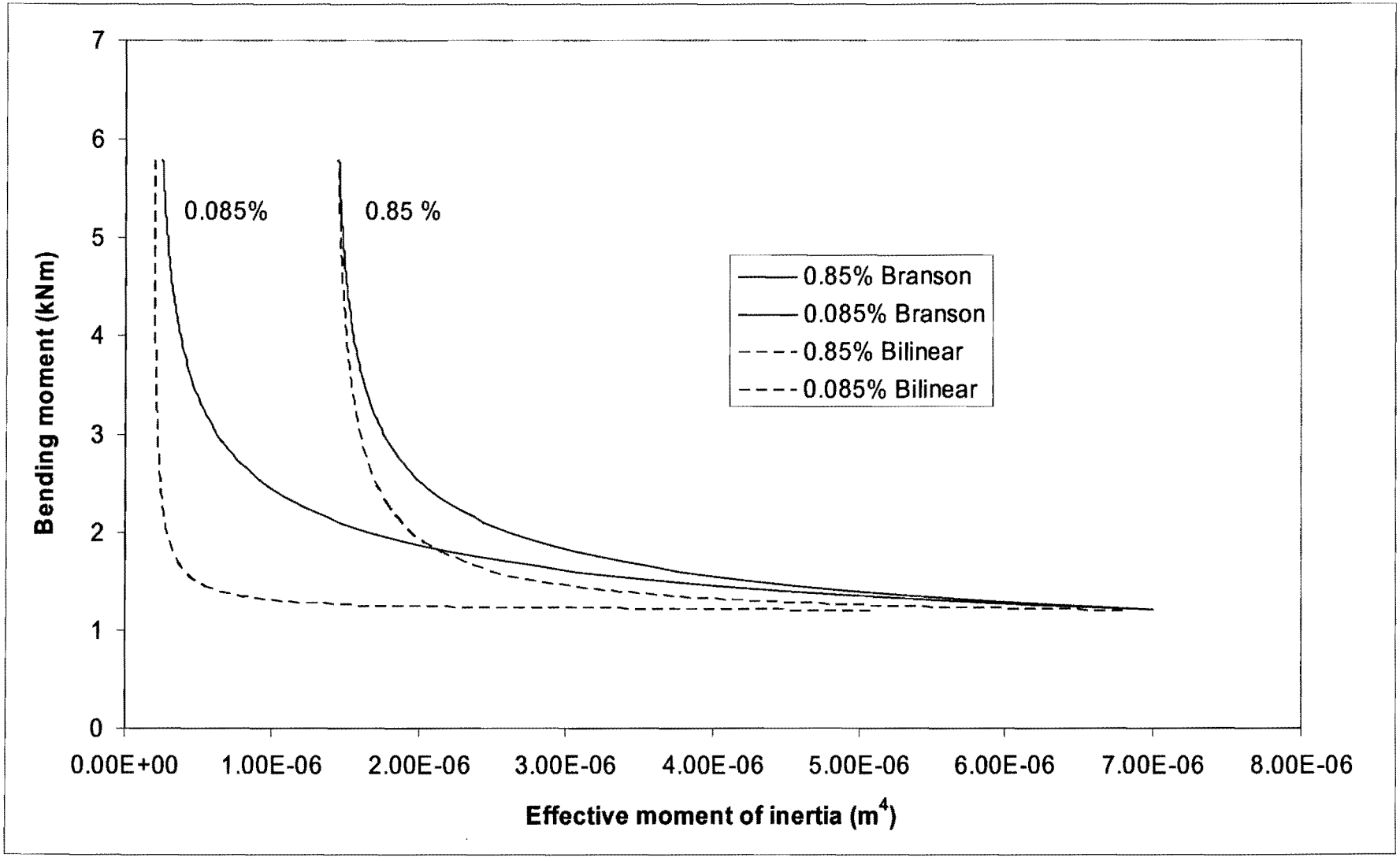

Figure 4-12: Comparison of the two tension stiffening methods

4.4 Haddad's Beam

The data for this beam test as well as the hand-calculation deflection results were obtained from Neville (1970). The cross sectional properties, layout and loading of the tested beam are illustrated in figure 4-13. It should be noted that the original test was carried out using imperial units.

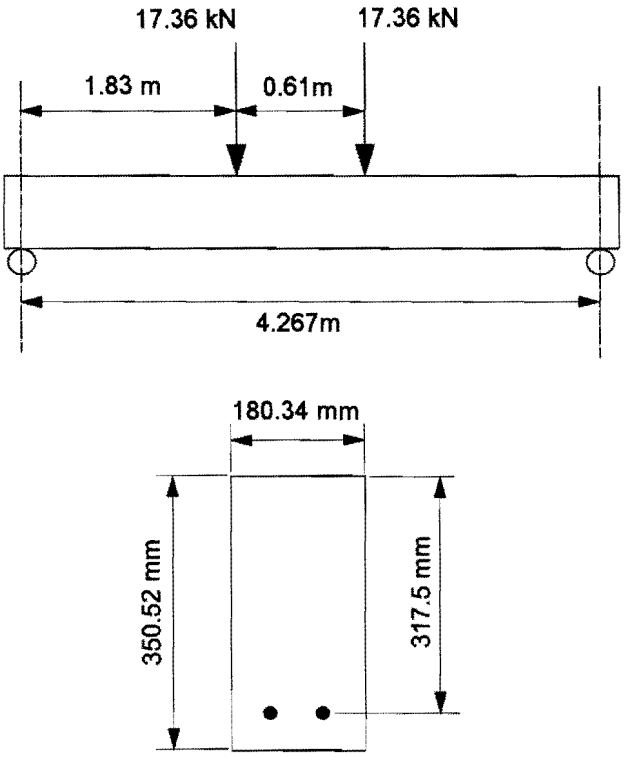

Figure 4-13: Geometry and loading of the beam tested by Haddad

Tabulated below are some material and geometric properties as established by Haddad:

Concrete cylinder strength, f_c'	26.34 MPa
Rupture modulus, f_r	3.1 MPa
Young's modulus, E	22.76 GPa
Free shrinkage strain, ε_{cs}	-204×10^{-6}
Creep coefficient, ϕ	2
Percentage tension reinforcement	1.42%

Table 4-3: Material properties of Haddad's beam

The rupture modulus was calculated, Neville (1970), from:

$$f_r = 0.6\sqrt{f_c'} \qquad (4.6)$$

The beam, modelled as a slab of the same width, was approximated with a 1x20 element mesh, as illustrated in figure 4-14. Three separate analyses were performed and compared with Haddad's experimental data as well as the results obtained by Neville with hand-calculation methods.

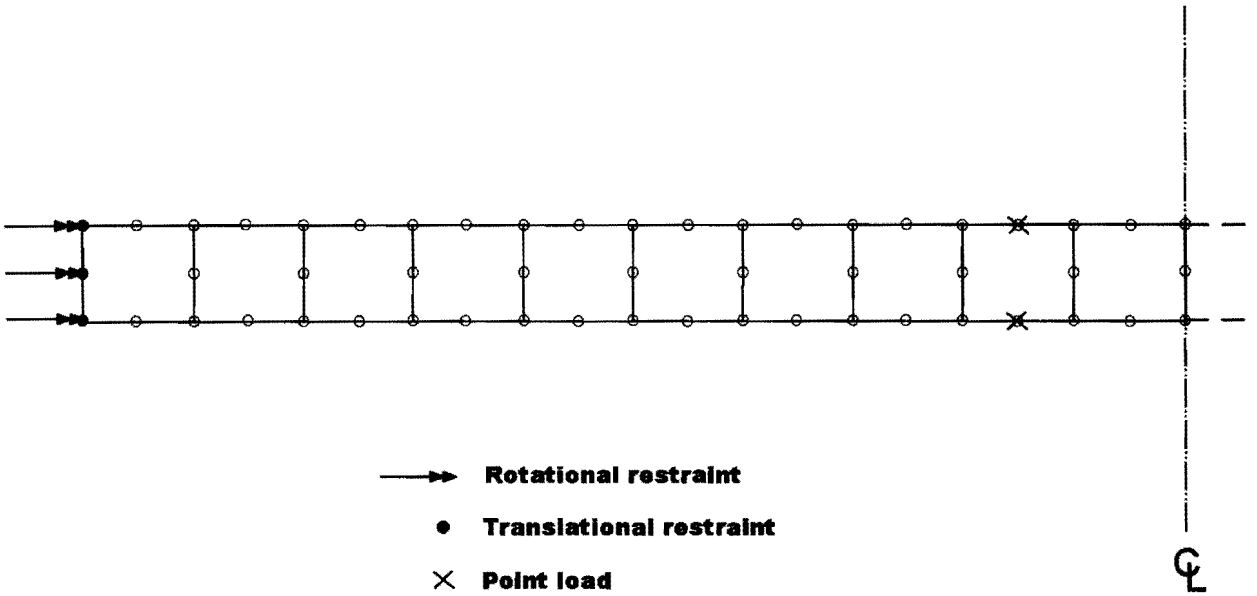

Figure 4-14: Plan view of the element layout

A simple elastic analysis, neglecting cracking and tension stiffening, yields a mid-span deflection of 3.67 mm which compares well with the value of 3.71 mm as predicted by analytical methods.

The table below compares the mid-span deflections at time infinity of the finite element analysis, Neville's results and Haddad's data.

	FEA (mm)	**Neville (mm)**	**Haddad (mm)**
Elastic with cracking (Branson)	5.8	5.28	5.84
Creep with cracking	3.14	3.81	
Shrinkage	1.28	1.04	
Total long term	10.22	10.13	10.9

Table 4-4: Comparison between the proposed model, Neville and Haddad's results

It should be noted that the method proposed in this dissertation assumes that the principle of superposition applies to the four stated components of time dependent deflection: elastic, cracked, shrinkage and creep.

The table indicates that the finite element analysis correlates extremely well with both the hand calculation methods employed by Neville and the actual results obtained by Haddad.

4.5 Simplified Analysis of a Slab Panel

As a further verification, a slab panel analysed with the hand-calculation method set out in section 2.1.1 is compared with the proposed finite element method. This panel is taken from Ghali and Favre (1986) and the detail is given below and in figure 4-15.

For the purposes of the hand calculation it is assumed that the moments and required reinforcement are known and only the final, long-term deflection is sought. Naturally, for the finite element approach, only slab geometry, required reinforcement and material properties are needed.

The panel is loaded with a uniformly distributed load q = 8.42 kN/m² on a 7m x 7m span. The depth of the slab, h = 200mm, and the average effective depth of the tension reinforcement in the x and y directions, d_t = 160mm. The modulus of elasticity at the time of loading E_c = 25GPa with the creep and aging coefficients $\phi(t, \tau)$ = 2.5 and $\chi(t, \tau)$ = 0.8, respectively. The modulus of rupture is given as f_r = 2MPa and the modulus of elasticity of the reinforcement E_s = 200GPa.

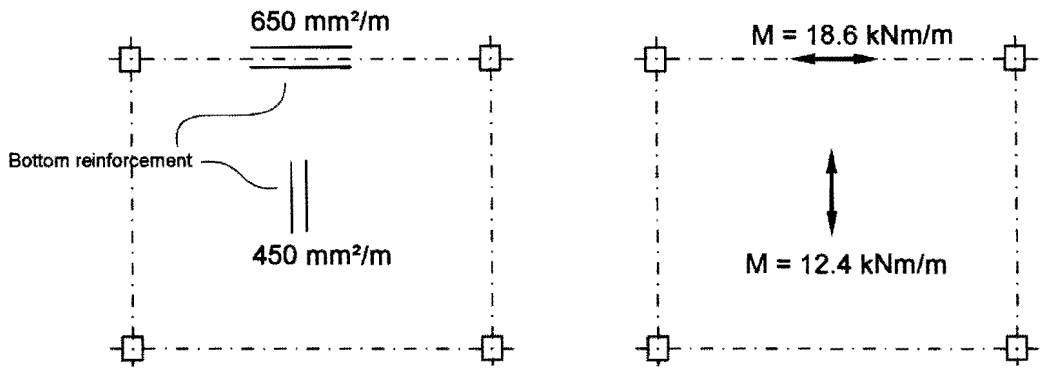

Figure 4-15: Reinforcement layout and moments of the slab panel

Top reinforcement is conspicuous in its absence in the figure above, and the assumptions made for the finite element analysis are elaborated upon in section 4.5.2. The hand calculation method on the other hand, oddly neglects the influence of negative reinforcement and cracking at the column supports.

4.5.1 Hand Calculation

The calculation in this sub-section is taken directly from Ghali and Favre (1986).
Equation (2.7) yields an uncracked moment of inertia, neglecting reinforcement as,

$$I_g = \frac{0.2^3}{12(1-0.2^2)} = 694\text{x}10^{-6}\text{m}^4/\text{m}$$

Using a deflection coefficient table based on equation (2.1) Ghali and Favre (1986), D, δ_{EF} and δ_{AB} are calculated as:

$$D = 0.00482\frac{ql^4}{E_cI_g} = 5.6mm$$

$$\delta_{AB} = 0.00342\frac{ql^4}{E_cI_g} = 3.97mm$$

$$\delta_{EF} = D - \delta_{AB} = 1.63mm$$

Column strip crack curvature coefficients are calculated using equations (2.46), (2.47) and interpolated with equation (2.48):

$$\kappa_{s1} = \frac{I_g}{I_1} = 0.98$$

$$\kappa_{s2} = \frac{I_g}{I_2} = 7$$

The cracking moment and the crack interpolation coefficient are calculated as:

$$M_r = \frac{f_rI_g}{y} = 13.33kNm/m$$

$$\zeta = 1-\beta_1\beta_2\left(\frac{M_r}{M}\right)^2 = 0.74 \quad \text{with } \beta_2 = 0.5 \text{ for long-term loading.}$$

The effective crack coefficient and cracked mid-span column strip deflection is then:

$$\kappa_s = (1-\zeta)\kappa_{s1} + \zeta\kappa_{s2} = 5.45$$

$$\delta_{AB} = 5.45 \times 3.97 = 21.65mm$$

The creep curvature coefficients are found using equation (2.64) and interpolated in a similar manner to calculate an ultimate creep deflection of 9.55mm. The middle strip deflections can be calculated in the exact same manner, Tables 4.5, 4.6 and 4.7 summarise the results of the comparison.

4.5.2 Finite Element Analysis

The finite element model consists of a 6x6 element mesh with the corners fixed against all displacements and the edges fixed against rotation about an axis parallel to the edge as shown in figure 4-16.

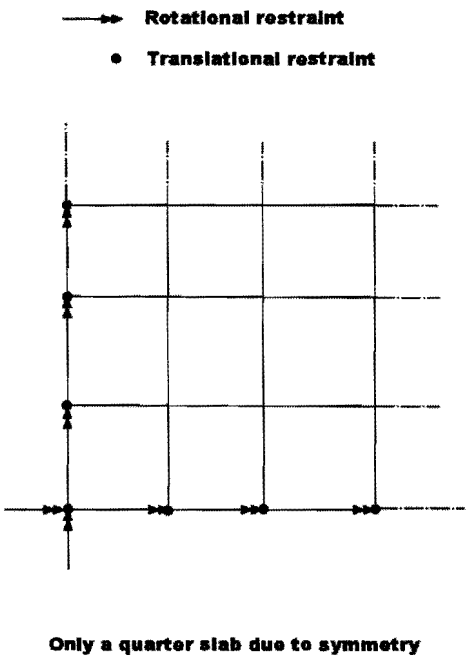

Figure 4-16: Finite element model

For the purposes of the finite element analysis, symmetric double reinforcement (top and bottom) is assumed as shown in figure 4-17.

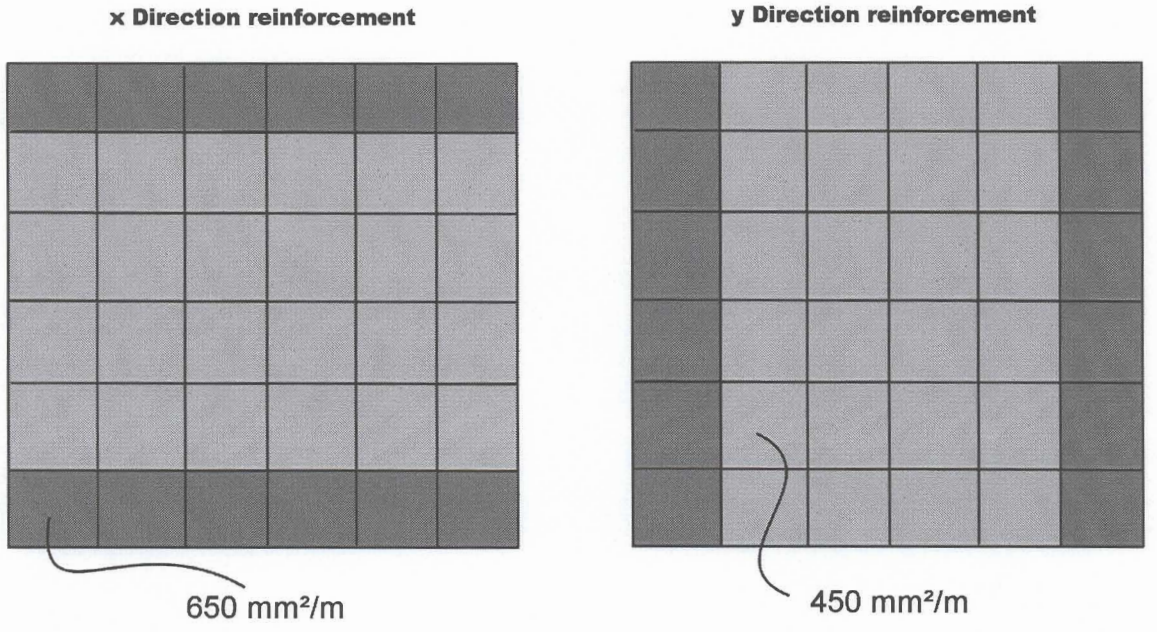

Figure 4-17: Assumed reinforcement layout

An uncracked, elastic finite element analysis yields a total mid-panel deflection, $D = 6.97$mm and a mid-column strip deflection $\delta_{AB} = 5.27$mm, compared to 5.6mm and 3.97mm as calculated in the preceding section.

The results for long-term cracked deflection and creep deflection are set out in the tables below.

	Hand calculation (mm) (Ghali & Favre, 1986)	**FEA (mm)**
Cracked: Branson		29.73
Cracked: Bilinear	21.65	36.28
Creep: Branson		5.56
Creep: Bilinear	9.55	6.44
Total: Branson		35.29
Total: Bilinear	31.2	42.72

Table 4-5: Column strip deflections

	Hand calculation (mm) (Ghali & Favre, 1986)	**FEA (mm)**
Cracked: Branson		2.08
Cracked: Bilinear	1.6	2.26
Creep: Branson		2.56
Creep: Bilinear	3.04	2.74
Total: Branson		4.64
Total: Bilinear	4.64	5

Table 4-6: Relative middle strip deflections

	Hand calculation (mm) (Ghali & Favre, 1986)	**FEA (mm)**
Cracked: Branson		31.81
Cracked: Bilinear	23.25	38.54
Creep: Branson		8.12
Creep: Bilinear	12.59	9.18
Total: Branson		39.93
Total: Bilinear	35.84	47.72

Table 4-7: Total mid-panel deflections

It is clear that use of the bilinear method consistently results in a higher deflection than is the case when Branson's method is employed. When viewed in the light of the discussion in section 4.3, it must be said that the bilinear method is unsuited for the purposes of this dissertation.

4.6 Cardington Slabs

A full scale seven storey concrete frame was erected and investigated at the BRE's (Building Research Establishment) Large-Building Test Facility in Cardington in the UK as part of the European Concrete Building project. The floors consists of flat slabs and deflection measurements were published by Vollum & Hossain (1998).

The publications concerning this building do not mention the exact reinforcement ratios but the project brief, Chana et al. (1998), contains enough data, table 4-8, to infer the designed reinforcement from a design calculation to Eurocode 2.

Parameter	Value
Dead load (Load combination factor)	5 kPa (1.35)
Live Load (Load combination factor)	2.5 kPa (1.5)
Panel dimensions	7.5m x 7.5m x 250mm
Column dimensions (Internal)	400mm x 400mm x 3.75m
Concrete	C37

Table 4-8: Cardington slabs parameters

A design calculation utilising the equivalent frame method, yields required reinforcement in the order of 360mm²/m for both the hogging and sagging moment regions. This reinforcement area and the parameters shown in Table 4-9 and Table 4-10, are used to calculate the long-term deflection with the method proposed by the author. The finite element mesh used is identical to that of figure 4-16 and the reinforcement shown in figure 4-17 is modified to 360mm²/m.

Parameter	Value
t_0, t_1, t_2, t_3 (Time)	2 days, 12 days, 300 days, 1000 days
w_0, w_1, w_2 (Sustained service load)	6.75 kPa, 10.7 kPa, 9kPa
E_0, E_1, E_2 (Modulus of elasticity)	27GPa, 33GPa, 33GPa
f_{r0}, f_{r1}, f_{r2} (Modulus of rupture)	2.7MPa, 3.6MPa, 3.6MPa
Concrete	C37, (35MPa)

Table 4-9: Cardington time dependent slab parameters

Time (days)	$\phi(t,t_0)$	$\phi(t,t_2)$
$t_0 = 2$	0	-
$t_1 = 12$	0.57	-
$t_2 = 300$	1.42	0
$t_3 = 1000$	1.72	1.03

Table 4-10: Creep coefficients

Two analyses were performed:

- FEA (2 steps) – In this analysis, creep deflection was calculated using properties from t_0 to t_2 in the first step, and a second step calculated creep deflections from t_2 to t_3. The first step used the 6.75kPa load and the second step 9kPa.
- FEA (1 step) – Here creep deflection was calculated in a single step from t_0 to t_3 using 9kPa.

The measured deflections are plotted against the results of the finite element analysis in figure 4-18.

The finite element analysis correlates well with the experimental data up to the application of the 9kPa load at t = 300 days. It is clear that the load history is of great importance when calculating long-term deflections and that the proposed method does not perform extremely well when faced with varying load histories. This problem would be exacerbated were the sustained load to decrease at any time, since full creep recovery would erroneously be shown by the proposed method.

Despite these failings, the method predicts the 1000 day creep deflection within +12% when load history is included and within -40% when load history is neglected.

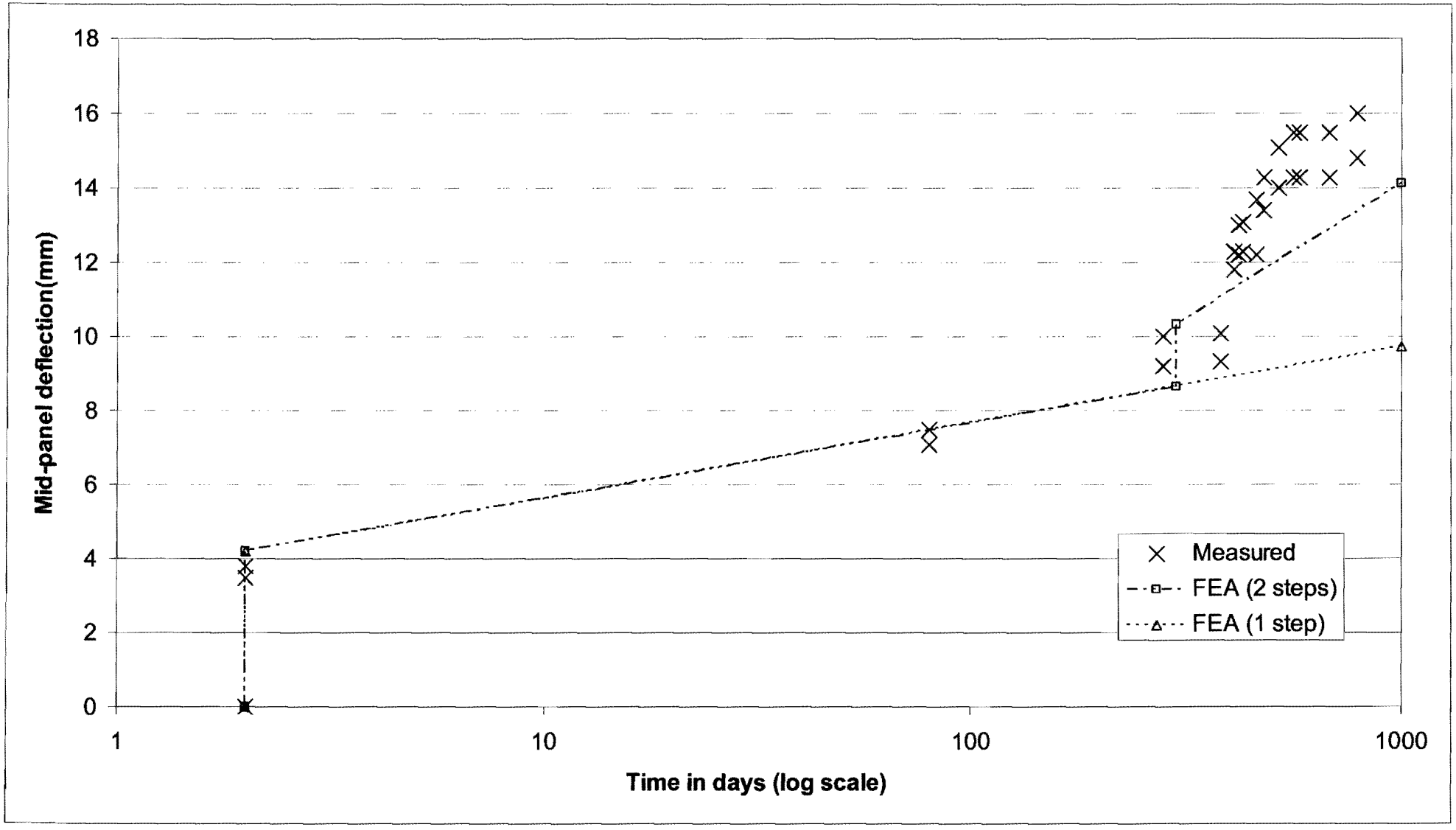

Figure 4-18: Finite element analysis plotted on the Cardington data